

## The Disintegration of $\text{Co}^{55}$ and $\text{I}^{130}$ †

ROBERT S. CAIRD AND ALLAN C. G. MITCHELL  
*Physics Department, Indiana University, Bloomington, Indiana*  
 (Received December 2, 1953)

The nuclear spectra of  $\text{Co}^{55}$  (18 hr) and  $\text{I}^{130}$  (12.6 hr) have been studied with the help of a magnetic lens spectrograph, a coincidence lens, and scintillation counters.  $\text{Co}^{55}$  emits gamma rays having energies 0.477, 0.935, 1.41, 0.253, 1.84, and 2.17 Mev, the last three being quite weak; and four beta-ray groups of energies 1.50, 1.03, 0.53, and 0.26 Mev with relative abundances of 53.3, 39.5, 4.9, and 2.3 percent, respectively. A disintegration scheme is proposed.  $\text{I}^{130}$  emits gamma rays of energy 0.409, 0.528, 0.660, 0.744, and 1.15 Mev together with two beta-ray groups of energies 1.02 and 0.597 Mev. The energy-level scheme is discussed in the light of the collective model.

### INTRODUCTION

THE spectra of  $\text{Co}^{55}$  and  $\text{I}^{130}$  have been studied some years ago by the use of the conventional methods of nuclear spectroscopy. The measurements of Deutsch and Hedgran<sup>1</sup> indicated that the main method of decay of  $\text{Co}^{55}$  occurs by the emission of two positron groups of energies 1.50 and 1.01 Mev together with the emission of three gamma rays of energies 0.47, 0.935, and 1.41 Mev. They also reported a weak gamma ray of energy 0.095 Mev which does not fit into the scheme.

The spectrum of  $\text{I}^{130}$  was studied by Roberts, Elliott, Downing, Peacock, and Deutsch<sup>2</sup> in the early days of nuclear spectroscopy. They showed that  $\text{I}^{130}$  decays by the emission of two beta-ray groups of energies 1.03 and 0.61 Mev together with four gamma rays whose energies are 0.417, 0.537, 0.667, 0.714 Mev. According to these authors the position of the gamma ray at 0.417 Mev is established from the energies of the two beta-ray groups but the remaining three gamma rays are all in cascade and their arrangement is arbitrary. Smith, Mitchell, and Caird<sup>3</sup> measured the spectrum of  $\text{Cs}^{130}$ , which also goes to  $\text{Xe}^{130}$ , with the hope of establishing the order of the gamma rays in cascade, but found that

these gamma rays were not excited in the disintegration of  $\text{Cs}^{130}$ .

Since a coincidence lens has recently been put into operation in this laboratory, it was felt that  $\text{Co}^{55}$  and  $\text{I}^{130}$  would be suitable subjects for investigation since each appears to disintegrate with the emission of two groups of nuclear particles followed by suitably separated gamma rays. In addition, the spectra of the two elements were investigated with the help of a conventional magnetic lens, and also using scintillation counters. As a result of the investigation, certain new features of the decay schemes of each nuclide have been discovered.

### THE COINCIDENCE LENS

One of the magnetic lenses in the laboratory was converted into a coincidence lens in which coincidences between gamma rays, detected by a scintillation counter and resolved in energy by a differential pulse-height analyzer, and beta rays, resolved magnetically by the lens, are measured. The lens which was used was that described by Bunker, Canada, and Mitchell.<sup>4</sup> A schematic of the arrangement of counters and electronic components is shown in Fig. 1.

The end plate of the instrument nearest the source was refitted to permit the insertion of a canned NaI(Tl) crystal and a lucite "light-piper" immediately behind the source. The NaI(Tl) crystal was in the form of a cylinder 1 in. in diameter by 1 in. high. The "light-piper" was  $4\frac{1}{2}$  in. long. Optical contact between the crystal, "light-piper," and a 5819 photomultiplier tube was made with the help of silicone grease. In order to minimize the effect of the magnetic field of the lens on the photomultiplier tube a solenoid was constructed, which was operated in parallel with the main coils of the lens. Thus, for any current in the main coils, the field at the photomultiplier was essentially zero.

Beta rays were detected at the other end of the lens with the help of a NaI(Tl) crystal in the form of a cube 1 cm on each edge. A "light-piper," 5819 photomultiplier tube, and solenoid, similar to those already described, were employed. The crystal was mounted *in vacuo* by clamping it to a Lucite window which was

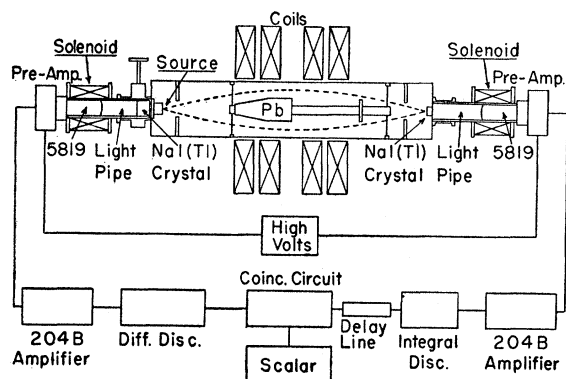


FIG. 1. Schematic diagram of coincidence lens.

† Supported by the joint program of the U. S. Office of Naval Research and the U. S. Atomic Energy Commission.

<sup>1</sup> M. Deutsch and A. Hedgran, *Phys. Rev.* **75**, 1443 (1949).

<sup>2</sup> Roberts, Elliott, Downing, Peacock, and Deutsch, *Phys. Rev.* **64**, 268 (1943).

<sup>3</sup> Smith, Mitchell, and Caird, *Phys. Rev.* **87**, 454 (1952).

<sup>4</sup> Bunker, Canada, and Mitchell, *Phys. Rev.* **79**, 610 (1950).

fitted with a rubber gasket to hold the vacuum. Optical contact was made between the crystal, Lucite "light-piper," and photomultiplier tube.

The general layout of the electronic equipment is shown in Fig. 1. The output of each photomultiplier goes through a cathode-follower preamplifier and from there into an Atomic Instrument Company Model 204B linear amplifier. In the beta-ray channel, the integral discriminator on the linear amplifier is used to cut down the noise and shape the pulses. The output then goes through a delay line to the coincidence circuit. In the gamma-ray channel, the output of the linear amplifier is fed to an Atomic Instrument Company Model 510 single-channel pulse-height analyzer. That portion of the pulse spectrum which is selected by the analyzer goes on to the coincidence circuit. The coincidence analyzer consists of suitable pulse-shaping

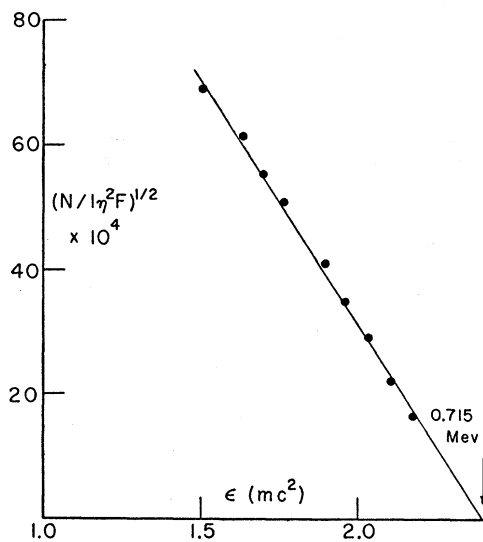


FIG. 2. Interior beta-ray group from  $\text{Rb}^{86}$  observed with coincidence lens.

devices, a diode discriminator, and amplifying stage, and an integral discriminator. The coincidence circuit was usually run at 0.20-microsecond resolving time. Either singles channel or the coincidence channel could be selected by a three-position switch and the output fed into a fast (1-microsecond dead time) decade scalar. The coincidence system was lined up by using a double pulse generator, putting simultaneous pulses into each of the cathode followers, and adjusting the delay line until true coincidences were obtained.

The singles system was calibrated by measuring the beta-ray spectrum and the internal conversion line from  $\text{Cs}^{137}$  with the lens and the beta counter. For the adjustments used, the resolution was about 6 percent. The gamma-ray counter was likewise calibrated using the  $\text{Cs}^{137}$  source. The full width at half-maximum for this line was about 15 percent.

The coincidence apparatus was tested by measuring

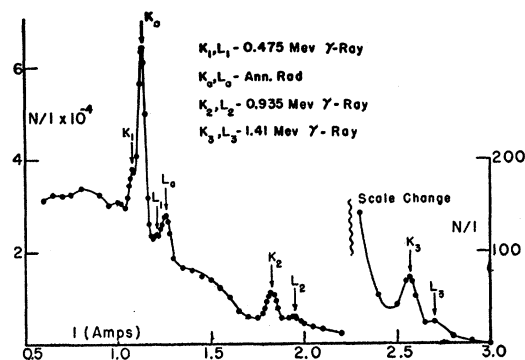


FIG. 3. Photoelectrons ejected by gamma rays from  $\text{Co}^{55}$  (Pb radiator).

the main spectrum of  $\text{Au}^{198}$  and the interior spectrum of  $\text{Rb}^{86}$ . In the case of  $\text{Au}^{198}$ , the scintillation counter at the gamma ray end was adjusted to accept the 0.411-Mev line, the beta-ray distribution in coincidence with this gamma ray was measured, and a Fermi plot in good agreement with the known decay scheme was obtained. In the case of  $\text{Rb}^{86}$ , the beta-ray distribution was measured using a single counter to obtain the shape and end point of the high-energy group. In addition, with the gamma-ray counter focused on the line at 1.08 Mev, the coincidence distribution was examined.

The Fermi plot for the interior group is shown in Fig. 2. Assuming an allowed shape for this group, the end-point energy is  $0.715 \pm 0.010$  Mev. The high-energy group exhibits the well-known shape characterized by  $\Delta j = \pm 2$  and a change of parity, and the end point being determined as 1.798 Mev. These results are in agreement with the work of Muether and Ridgeway<sup>5</sup> and the earlier work of Zaffarano, Kern, and Mitchell.<sup>6</sup>

#### Experiments on $\text{Co}^{55}$

$\text{Co}^{55}$  (18 hr) was prepared by bombarding iron with 11.5-Mev deuterons on the probe of the Indiana University cyclotron. With the exception of the 9-hour isomeric state of  $\text{Co}^{58}$ , which gives only low-energy internal conversion electrons, the only other cobalt isotopes produced are long-lived and suitable corrections can be made for them. A chemical separation was made on all source material. The purified cobalt was then examined for beta rays and gamma rays.

#### THE GAMMA-RAY SPECTRUM

The gamma-ray spectrum was measured in a magnetic lens spectrometer using both lead and uranium radiators. A typical spectrum, taken with a lead radiator of 12-mg/cm<sup>2</sup> surface density is shown in Fig. 3, in which the number of counts per momentum interval ( $N/I$ ), is plotted as a function of the current in the coils of the lens. All lines except one at 0.5 amp (not shown) decay

<sup>5</sup> H. R. Muether and S. L. Ridgeway, Phys. Rev. 80, 750 (1950).

<sup>6</sup> Zaffarano, Kern, and Mitchell, Phys. Rev. 74, 682 (1948).

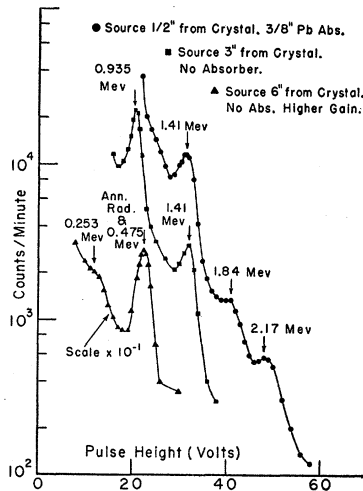


FIG. 4. Scintillation spectrum of gamma rays from  $\text{Co}^{55}$ .

with a period of 18 hours and are attributed to  $\text{Co}^{55}$ . The line at 0.5 amp (an  $L$  line for a gamma ray of 0.119 Mev), decays with a much longer period and is attributed<sup>7,8</sup> to  $\text{Co}^{57}$ . The line at 0.475 Mev is not well resolved from annihilation radiation. In order to resolve these two lines and to get an estimate of the relative intensity of the line at 0.475 Mev with respect to the others, a lead radiator of 7.75-mg/cm<sup>2</sup> surface density was employed and the region around 0.500 Mev was studied carefully. The energies and relative intensities of the gamma rays, and the abundances per positron of the lines, are given in Table I. The results for the strong lines are in reasonable agreement with those of Deutsch and Hedgran.<sup>1</sup>

As a result of the measurement of the energy distribution of the positrons (see below), two weak positron groups were found in addition to the two main groups reported by Deutsch and Hedgran. These two groups had lower energies than the two main groups. In order to look for low-intensity gamma rays connected with the emission of these positron groups, the gamma rays

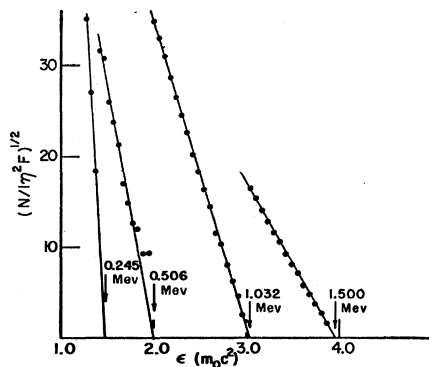


FIG. 5. Fermi plot of positron groups from  $\text{Co}^{55}$ .

<sup>7</sup> Cheng, Dick, and Kurbatov, Phys. Rev. 88, 887 (1952).

<sup>8</sup> L. G. Elliott and M. Deutsch, Phys. Rev. 64, 321 (1943).

were investigated with the help of a scintillation spectrometer. The scintillation spectrometer consisted of a 1-in. cylindrical NaI(Tl) crystal together with a Dumont 6292 photomultiplier tube. After appropriate amplifications the pulses were analyzed using a single channel pulse height analyzer. The instrument was calibrated with the help of the  $\text{Cs}^{137}$  and  $\text{Co}^{60}$  gamma rays.

In searching for the higher-energy gamma rays, a  $\frac{3}{8}$ -inch lead absorber was used to absorb the lower-energy gamma rays. This prevented "pulse pileup" from contributing to the general background in the high-energy region. The low-energy region, of course, was measured without lead absorber. The results are shown in Fig. 4. The strong lines found in the magnetic spectrometer were found in the scintillation spectrometer together with three additional lines at 2.17, 1.84, and 0.253 Mev. Owing to the weakness of the lines and the decrease of photoelectric cross section with energy, strong sources had to be used to locate and measure the intensity of the higher-energy lines. The usual

TABLE I. Summary of energies and intensities of gamma-rays.

Line energy Mev	$\text{Co}^{55}$ Strong lines		Deutsch and Hedgran
	$I/I_a$	$I/\text{positron}$	
0.477	0.14	0.28	0.3
AnnRad	1.00	1.00	...
0.935	0.78	1.56	1.4
1.41	0.13	0.26	0.3
	Weak lines		
0.253	0.01	0.02	
1.84	0.003	0.006	
2.17	0.02	0.04	

precautions such as change of solid angle, change of absorber, and measurement of the period, were taken to make sure that the peaks were genuine and not due to pulse addition.

Owing to the large difference in intensity between the strong lines and the weak lines, a series of comparisons had to be made using various sources and different experimental arrangements. For example, the lines at 1.41, 1.84, and 2.17 Mev were compared using a strong source and the lead absorber, corrections being made for the absorber. The line at 0.935 Mev was then compared with that at 1.41 Mev using no absorber. Finally, the lines at 0.935, 0.510 and 0.477, and 0.253 were compared using a weaker source. The results of the measurements are shown in Table I. It is felt that the relative intensities of the weak lines give an order of magnitude only.

#### THE PARTICLE SPECTRUM

The particle spectrum—positrons and internal conversion electrons—was investigated with the help of three different magnetic spectrometers—a magnetic

lens, the coincidence lens, and a  $180^\circ$  spectrometer. Preliminary experiments gave indications of positron groups of lower energy than the two main groups reported by Deutsch and Hedgran. A careful investigation was made of the particle spectrum in the magnetic lens using a counter window which would transmit particles down to less than 10 keV. The source, made by evaporating active cobalt chloride onto a thin aluminum backing, was  $0.5 \text{ mg/cm}^2$  thick. Aside from the  $\text{Co}^{55}$  spectrum, two internal conversion lines of long period having energies of 120 and 134 keV,  $K$  and  $L$  lines for a gamma ray of 23-keV energy, and  $K$  lines for gamma rays of 72- and 95-keV energy having half-lives of approximately 9 hours were seen. The lines from the gamma rays at 120 and 134 keV presumably arise from the 270-day<sup>9</sup>  $\text{Co}^{57}$  and those from the gamma ray at 23 keV from the isomeric transition<sup>9</sup> of  $\text{Co}^{58}$ . The lines at 72 and 95 keV, having a period of 9 hours, may also be connected with the decay of  $\text{Co}^{58}$ , but further work is necessary to establish this.

The data were corrected for small amounts of any other cobalt activities, and a Fermi plot made. The results are shown in Fig. 5 and the end points, relative abundances, and values of  $\log ft$  are shown in Table II.

TABLE II. Positron groups from  $\text{Co}^{55}$ .

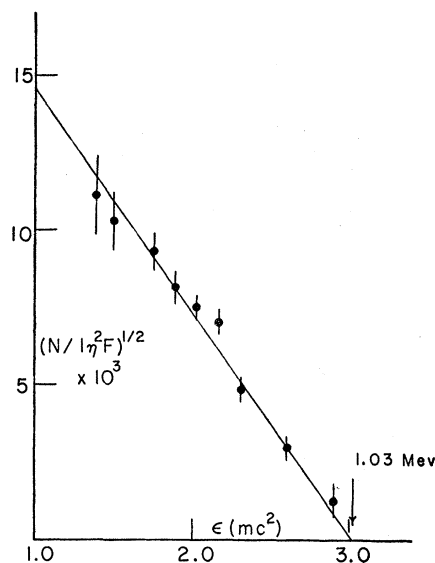
$E(\text{Mev})$	Abundance percent	$\log ft$
$1.500 \pm 0.008$	53.3	6.3
$1.03 \pm 0.03$	39.5	5.8
$0.53 \pm 0.03$	4.9	5.9
$0.26 \pm 0.02$	2.3	6.0

It will be seen that, in addition to the two main positron groups at 1.50 and 1.03 MeV, there are two weak groups at 0.53 and 0.26 MeV. A similar experiment made with a  $180^\circ$  spectrometer, to investigate the internal conversion lines of  $\text{Co}^{55}$ , gave results in agreement with those given above. The values given in Table II are the averages of all the experiments.

An experiment was then made with the coincidence lens. The scintillation spectrometer was set on the high-energy side of the peak of the 1.41-MeV gamma ray and those positrons which were in coincidence were measured. The end point obtained from a Fermi plot of this spectrum, shown in Fig. 6, is 1.03 MeV. The weak low-energy groups are not shown.

Finally, the internal conversion of the strong lines at 0.477, 0.935, and 1.41 MeV were investigated in a  $180^\circ$  spectrograph. The intensity of the internal conversion lines were found to be  $1.10 \times 10^{-4}$ ,  $1.24 \times 10^{-4}$ , and  $3.53 \times 10^{-5}$  internal conversion electrons per positron for the lines in order of increasing energy.

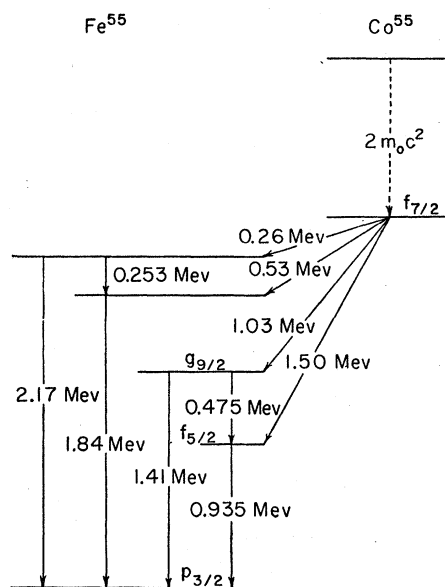
<sup>9</sup> Nuclear Data, National Bureau of Standards, Circular No. 499 (U. S. Government Printing Office, Washington, D. C., 1950).

FIG. 6. Fermi plot of second group of positrons in  $\text{Co}^{55}$  taken with coincidence lens.

## CONCLUSIONS

The results of the investigation are embodied in the decay scheme shown in Fig. 7. The strong gamma rays at 0.477, 0.935, and 1.41 MeV, together with the strong positron groups at 1.50 and 1.03 MeV, constituting the principal mode of decay, are in agreement with the work of Deutsch and Hedgran.<sup>1</sup>

The present experiments show two new positron groups at 0.53 and 0.26 MeV together with additional weak gamma rays. If the strong gamma rays and the positron groups are used to establish the energies of the levels, the weak gamma rays agree both in energy

FIG. 7. Disintegration scheme for  $\text{Co}^{55}$ .

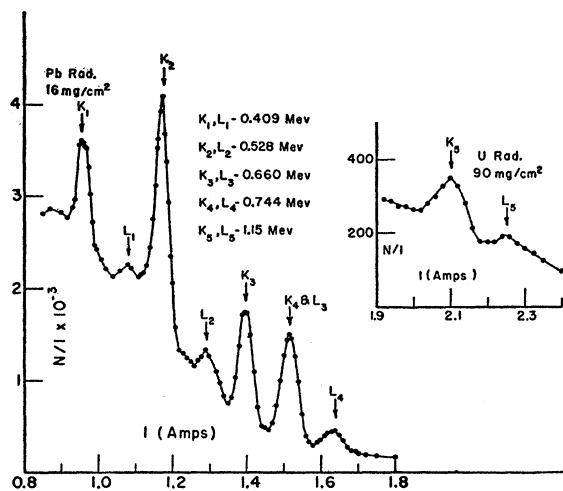


FIG. 8. Photoelectrons ejected by gamma rays from  $I^{130}$ .

and intensity with the transitions as shown in the level scheme. Two other possible gamma rays involving transitions from the state at 1.90 Mev to those at 1.41 and 0.938 Mev were not seen. The first of these transitions would be obscured by the annihilation radiation and the second by the line at 0.938 Mev.

According to the shell model, the single particle level for the ground state of  $^{55}_{27}\text{Co}$  is  $f_{7/2}$  and for the ground state of  $^{55}_{26}\text{Fe}$  is  $p_{3/2}$ . Thus it appears reasonable that no positron transition takes place to the ground state of the product. The level order in  $\text{Fe}^{55}$  should be  $p_{3/2}$ ,  $f_{5/2}$ ,  $g_{9/2}$ . The experimentally determined value of  $\log ft$  for the 1.50-Mev positron group is 6.3 and appears to be somewhat high for a  $f_{7/2}$  to  $f_{5/2}$  transition. The value of  $\log ft$  for the 1.03-Mev group is 5.8 and is in good agreement with what would be expected for a  $f_{7/2}$  to  $g_{9/2}$  transition. It is not felt that the determination of the internal conversion coefficients, either by the present writers or by Deutsch and Hedgran, is accurate enough to be of much help in determining the character of the states involved.

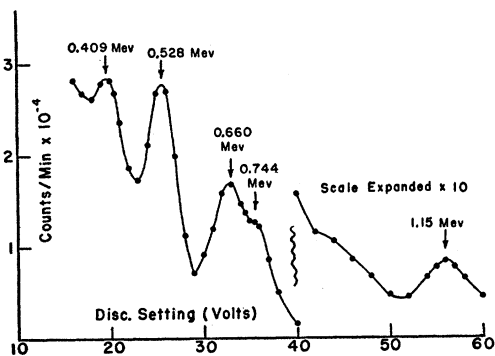


FIG. 9. Scintillation spectrum of gamma rays from  $I^{130}$ .

### Experiments on $I^{130}$

$I^{130}$  was prepared by bombarding tellurium with deuterons. The sample was dissolved in  $\text{HNO}_3$  with some KI, to serve as a carrier, and the iodine was distilled off, extracted by  $\text{CCl}_4$  and eventually precipitated as AgI for use as sources. The  $I^{130}$  (half-life 12.6 hrs) was accompanied by other iodine activities and corrections for these had to be made in doing the experiments. In order to keep unwanted activities to a minimum, separated  $\text{Te}^{130}$  was used as a target for some experiments.

### THE GAMMA RAYS

In order to investigate the gamma rays, the spectrum of the photoelectrons ejected from either a lead or a uranium radiator was measured in a magnetic lens spectrograph. The main curve of Fig. 8 shows the number of photoelectrons per unit momentum interval for a lead radiator of  $16 \text{ mg/cm}^2$  surface density plotted against the current in the lens. The peaks labelled  $K_1, L_1$ , to  $K_4, L_4$ , denote the  $K$  and  $L$  photoelectric peaks arising from four different gamma rays emitted by  $I^{130}$ . The peak labelled  $K_4 + L_3$  contains the  $K$  photoelectrons for a line at 0.744 Mev and the  $L$  peak for a line at 0.660 Mev. A similar experiment with a uranium radiator resolved the  $K_4$  from the  $L_3$  peak but caused the overlapping of other lines. The energies of these lines are given in Table III.

The gamma rays were also measured using a NaI(Tl) scintillation spectrometer and the results are shown in Fig. 9. In this figure, the two low-energy lines shown in Fig. 9 are clearly resolved but the line at 0.660 Mev shows some overlapping with that at 0.744 Mev. In addition a higher-energy line of energy about 1.15 Mev is seen. Experiments were performed to be sure that this line was not due to "pulse pileup." The spectrum was then reinvestigated in the magnetic lens spectrometer employing a strong source and a uranium radiator. The result is shown in the insert of Fig. 8 where a  $K$  and an  $L$  photopeak will be seen corresponding to a line at 1.15 Mev.

Estimates of the relative intensities of the gamma rays were obtained by determining the area under the several  $K$  photopeaks involved and applying the corrections for the variation of photoelectric efficiency with energy. Since the  $K$  photopeak for the line at 0.744 and the  $L$  photopeak for the line at 0.660 coincide, a correction had to be made for the intensity of the

TABLE III. Gamma rays from  $I^{130}$ .

Gamma ray	Energy of gamma ray Mev	Relative intensity
1	0.409	0.3
2	0.528	1.00
3	0.660	0.9
4	0.744	0.8
5	1.15	0.4

latter. This was accomplished by measuring the *K* and *L* photopeaks for the line at 0.530 Mev and using this to compute the contribution of the *L* peak for the line at 0.660 Mev. The intensity of the line at 1.15 Mev was determined by comparing the *K* photopeak produced by it in a uranium radiator with those of the other lines produced by the same source using a uranium radiator. The results, shown in Table III, are not felt to be known to better than 20 percent.

### THE BETA-RAY SPECTRUM

The distribution of beta rays and internal conversion electrons was investigated with the help of the magnetic lens spectrometer. Figure 10 shows that part of the spectrum containing the internal conversion lines. All lines are internally converted. A Fermi analysis of the beta-ray spectrum was made and it was found to be resolvable into two groups with end-point energies of 1.02 and 0.597 Mev, in agreement with Roberts *et al.* No groups of higher energy than that at 1.02 Mev were found. Table IV gives the characteristics of the beta-ray groups.

The number of internal conversion electrons per disintegration were obtained by taking the area under the *K* internal conversion peaks and comparing this to the area under the beta-ray spectrum. For the line at 1.15 Mev the *L* line was not resolved from the *K* line. The results are given in Table V together with estimates of the *K/L* ratios.

### COINCIDENCE EXPERIMENTS

Two scintillation counters using NaI(Tl) crystals and equipped with differential pulse-height analyzers were used to measure coincidences between certain gamma-ray lines. The resolving time of the coincidence circuit was 0.2 microsecond.

Two sets of experiments were carried out. In the first one, Channel 2 was set on the high side of the peak arising from the (0.660+0.744)-Mev lines, and Channel 1 was swept through the range of the spectrum. Figure 11 shows the result of the experiment. It will be seen that the coincidence curve shows a peak at 0.660 Mev, somewhat to the lower energy side of the composite peak shown in the singles spectrum. Peaks are also seen for the 0.528- and 0.409-Mev lines in the coincidence spectrum.

A similar experiment was carried out in which Channel 1 was set on the line at 1.15 Mev and Channel 2 swept across the spectrum. The results show that the 1.15-Mev line is in coincidence with those at 0.660 and 0.528 Mev but not with those at 0.409 and 0.744 Mev.

TABLE IV. Beta rays from I<sup>130</sup>.

<i>E</i> Mev	Rel. abundance Percent	log <i>ft</i>
1.02	46	6.5
0.597	54	5.5

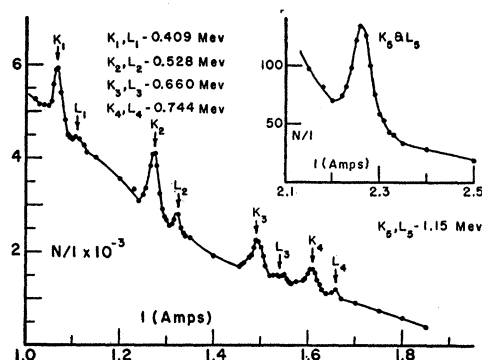


FIG. 10. Internal conversion lines from I<sup>130</sup>.

### DISCUSSION OF THE RESULTS ON I<sup>130</sup>

The present experiment has shown that, in addition to the gamma-ray lines established by Roberts *et al.*, there is an additional gamma ray having an energy of 1.15 Mev. The position of the line at 0.409 Mev is fixed by the difference in energy of the two beta-ray groups and is therefore placed at the top of the disintegration scheme in agreement with previous work. The existence of the line at 1.15 and the gamma-gamma coincidence experiments involving this line show that it must be in parallel with those at 0.409 and 0.744 Mev, which definitely fixes the position of the 0.744-Mev line. The other two lines are placed in cascade at the bottom of the scheme. Relative intensity determinations, although not very accurate, tend to confirm this assignment. The proposed decay scheme is shown in Fig. 12. The line at 0.528 Mev is placed below that at 0.660 Mev from considerations involving the collective model.

In order to obtain some idea of the spins and parities of the states involved, the internal conversion coefficients of the various lines have been calculated and compared with the values given by Rose, Goertzel, and Perry.<sup>10</sup> Since the lines at 0.528 and 0.660 Mev are in cascade and follow all beta and all other gamma transitions, the calculation is straightforward. In order to calculate the internal conversion coefficients for the other lines, the number of transitions per disintegration for the line in question must be calculated making use

TABLE V. Internal-conversion data.

<i>E<sub>γ</sub></i>	<i>K</i> internal-conversion electrons per disintegration	<i>K/L</i>	$\alpha_K$ (obs)	$\alpha_K$ (theor)
0.409	$4.4 \times 10^{-3}$	11	$1.6 \times 10^{-2}$	...
0.528	$5.5 \times 10^{-3}$	8	$5.5 \times 10^{-3}$	$6.8 \times 10^{-3}$ ( <i>E2</i> )
0.660	$3.2 \times 10^{-3}$	16	$3.2 \times 10^{-3}$	$3.8 \times 10^{-3}$ ( <i>E2</i> )
0.744	$2.1 \times 10^{-3}$	4	$2.7 \times 10^{-3}$	$2.9 \times 10^{-3}$ ( <i>E2</i> )
1.15	$(8.8 \times 10^{-5})^a$	..	$2.5 \times 10^{-4}$	$4.7 \times 10^{-4}$ ( <i>E1</i> )

<sup>a</sup> The number in parenthesis denotes that this of the total number of internal conversion electrons per disintegration.

<sup>10</sup> Rose, Goertzel, and Perry, Oak Ridge National Laboratory Report ONRL-1023, June 25, 1951, (unpublished).

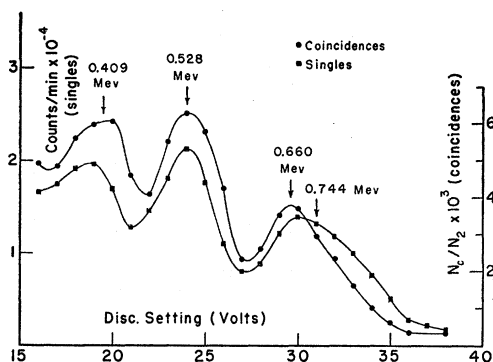


FIG. 11. Gamma-gamma coincidence experiment. (Channel 2 Set on the line at 0.744 Mev.)

of the assumed disintegration scheme, the relative abundance of the two-beta-ray groups, and the branching ratio for the gamma rays emitted from the state at 2.34 Mev. The branching ratio,

$$X = I_{0.407} / (I_{0.407} + I_{1.15}),$$

can be calculated either from the observed relative intensities of the lines at 0.407 and 1.15 Mev or from the relative intensities of the 0.407- and 0.744-Mev lines taking into consideration the relative abundance of the two beta-ray groups. The value for the branching ratio is  $X = 0.47 \pm 0.04$ . The number of transitions per disintegration involving the line at 0.744 Mev is therefore

$$N^{0.744} / N_{\text{dis}} = 0.54X + 0.46 = 0.79.$$

Taking into account the number of  $K$  internal-conversion electrons per disintegration given in Table V, the internal conversion coefficient can be calculated. A similar procedure was used for the other lines. The results together with the theoretical values are shown in Table V. The internal conversion coefficients for lines at 0.528, 0.660, and 0.744 Mev all agree with the theoretical prediction for  $E2$  radiation. The internal conversion coefficient of the 0.409- and 1.15-Mev lines are much less certain since their determination is very sensitive to the branching ratio  $X$ . The line at 1.15 Mev appears to be reasonably consistent with  $E1$  radiation, while that at 0.409 Mev might be  $E1$  ( $4.2 \times 10^{-3}$ ),  $E2$  ( $4.0 \times 10^{-2}$ ), or  $M1$  ( $1.74 \times 10^{-2}$ ). Since the ground state of  $\text{Xe}^{130}$  has zero spin and even parity, the  $E2$  character of the lines at 0.528, 0.660, and 0.744 Mev, suggests spins of 2, 4, 6, and even parity for the first three excited states. This is in agreement with what is to be expected from either the single-particle model for an even-even nucleus or from the collective model. The value of  $\log ft$  for the 1.02-Mev beta group would imply  $\Delta I = 0$ , yes for this transition.<sup>11</sup> Combining this information with that obtained for the first three excited states of  $\text{Xe}^{130}$ , the spin and parity of the ground state of  $\text{I}^{130}$  is 6, odd. The value of  $\log ft$  for the 0.597-

<sup>11</sup> L. W. Nordheim, *Revs. Modern Phys.* **23**, 322 (1950).

Mev group shows that it is allowed and is consistent with  $\Delta I = 1$ , no. The spin and parity of the state in  $\text{Xe}^{130}$  at 2.34 Mev would then have to be 5, odd, which is consistent with the  $E1$  character of the 1.15-Mev line. The internal conversion coefficient and relative intensity of the line at 0.409 Mev is still somewhat of an anomaly.

Since neither the parent nor the product nucleus corresponds to a case in which the proton or the neutron number is one less or one greater than a closed shell, the single-particle model is not strictly applicable. It is interesting to compare the present results with what would be expected on the basis of the collective model of Bohr and Mottelson.<sup>12,13</sup> They point out that in the region between closed shells, the strong-coupling collective model gives good results for the ratio of the energies of the lower excited states. The closer one approaches closed shells (magic numbers for protons or neutrons) the less appropriate the strong-coupling theory becomes. In the present instance both the parent and product are reasonably close to closed shells (50 protons and 82 neutrons). Nevertheless, the present experiments may serve as a test of the collective model.

For even-even nuclei with sufficiently great deformation, the collective model predicts a rotational spectrum of levels with energies:<sup>12</sup>

$$E_I = (\hbar^2/2J)I(I+1) + \Delta E_I; \quad I = 0, 2, 4, \dots, \quad (1)$$

in which  $J$  is the effective moment of inertia, and  $\Delta E_I$ , the first order correction to the strong-coupling formula, is given approximate y by

$$\Delta E_I = -2(\hbar\omega)^{-2}(\hbar^2/J)^2 I^2(I+1)^2. \quad (2)$$

Here  $\hbar\omega$  is the surface phonon excitation energy, about 2.2 Mev at  $A = 130$ . Equation (2) is the sum of Eq.

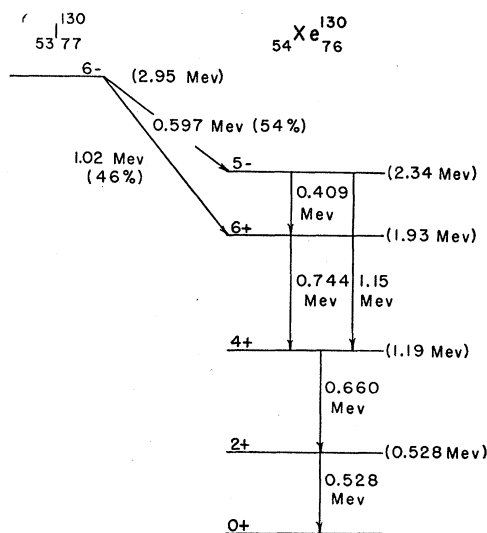


FIG. 12. Disintegration scheme of  $\text{I}^{130}$ .

<sup>12</sup> A. Bohr and B. R. Mottelson, *Kgl. Danske Videnskab. Selskab., Mat.-fys. Medd.* **27**, No. 16 (1953).

<sup>13</sup> A. Bohr and B. R. Mottelson, *Phys. Rev.* **90**, 717 (1953).

(VI 3a) and (VI 3b) of reference 12, in which  $\omega_\beta$  and  $\omega_\gamma$  have been replaced by limiting strong-coupling values.

One may check the rotational interpretation of the low states of  $\text{Xe}^{130}$  qualitatively in several ways: (1) the level order is consistent with the predicted order  $0+, 2+, 4+, 6+$ . (2) One can calculate the nuclear deformation from the energy of the first excited state using the relation<sup>14</sup>

$$\beta^2 = 171/A^{5/3}E_2(\text{Mev}). \quad (3)$$

The result is  $\beta = 0.310$ , which fits very well into the systematic trend of the other Xe isotopes,<sup>14</sup> suggesting a regularly decreasing nuclear deformation as the closed neutron shell at  $N=82$  is approached. (3) The ratios of the energies of the excited states,  $E_4/E_2$  and  $E_6/E_2$  deviate from the limiting strong coupling ratios in the expected direction, but the deviation is too large to receive quantitative explanation in terms of the

<sup>14</sup> K. W. Ford, Phys. Rev. **90**, 29 (1953).

TABLE VI. Energy ratios for excited states in  $\text{Xe}^{130}$ .

	Experiment	Theory	
		Without $\Delta E_I$	With $\Delta E_I$
$E_4/E_2$	2.25	3.33	1.94
$E_6/E_2$	3.66	7.00	...

first order correction given by Eq. (2). The comparison of theoretical and experimental ratios is shown in Table VI. It seems reasonable to interpret the  $\text{Xe}^{130}$  levels as collective rotations, but the nuclear deformation is not great enough to lend quantitative validity to the strong coupling approximation which works so well in the rare earth region and the region near uranium.

The authors are indebted to Dr. M. B. Sampson and the cyclotron group for making the bombardments, and to Mr. Arthur Lessor for making the chemical separations. They are also indebted to Dr. Kenneth W. Ford for many helpful discussions. The separated  $\text{Te}^{130}$  was obtained from the Oak Ridge National Laboratory.

## Angular Correlations in the $\text{Be}^9(d,p\gamma)\text{Be}^{10}$ and $\text{Be}^9(d,\alpha\gamma)\text{Li}^7$ Reactions\*

L. COHEN,† S. S. HANNA, AND C. M. CLASS‡

*Department of Physics, The Johns Hopkins University, Baltimore, Maryland*

(Received October 29, 1953)

The  $(d,p\gamma)$  correlation at  $E_d=0.84$  Mev was measured under the following conditions: (1) proton direction fixed at  $0^\circ$  to the deuteron beam, gamma direction varying, (2) proton direction fixed at  $90^\circ$  to the beam, gamma direction varying in the deuteron-proton plane, and (3) proton direction fixed at  $90^\circ$ , gamma direction varying in the  $90^\circ$  plane, perpendicular to the beam. The three correlations were different, and showed varying amounts of anisotropy. The appearance of terms in  $\cos^2\theta$  in these correlations indicates that the spin of the first excited state of  $\text{Be}^{10}$  is  $\geq 2$ . Coupled with other information on this state, this result gives a spin assignment of 2. A qualitative discussion of the correlations is given, and the effect of the deuteron stripping process is considered. The  $(d,\alpha\gamma)$  correlation was also measured with the alpha direction fixed at  $90^\circ$  to the beam and the gamma direction varying in the deuteron-alpha plane. Failure to detect a departure from isotropy again confirms the assignment of  $\frac{1}{2}$  to the spin of the first excited state of  $\text{Li}^7$ .

### I. INTRODUCTION

THE electromagnetic radiation from the first excited state of  $\text{Be}^{10}$  has been studied in coincidence with short-range protons in the reaction,  $\text{Be}^9(d,p)\text{Be}^{10*}(\gamma)\text{Be}^{10}$ . The coincidence yield in such a reaction is, in general, a function of considerable complexity, involving the directions of the deuteron, proton, and gamma ray, as well as the deuteron energy and the properties of the various states and particles taking part in the process. The correlation function will

be designated by  $W(\theta_p, \theta_\gamma, \phi)$ , where  $\theta_p$  and  $\theta_\gamma$  are measured with respect to the direction of the deuteron, and  $\phi$  is the dihedral angle between the proton-deuteron and gamma-deuteron planes, all in the center-of-mass coordinate system.

The following correlation functions were measured:

(1)  $W(0, \theta_\gamma, \phi) = W(0, \theta_\gamma)$ . If only waves of the same parity are present in the gamma-ray transition, as will be assumed henceforward, the correlation function has reflection symmetry in the  $\theta_\gamma = 90^\circ$  plane, and can be written:

$$W(0, \theta_\gamma) = \sum_{n=0}^K A_{2n} \cos^{2n}\theta_\gamma = W(0, 180 - \theta_\gamma),$$

\* Assisted by a contract with the U. S. Atomic Energy Commission.

† Now at Knolls Atomic Power Laboratory, General Electric Company, Schenectady, New York.

‡ Now at Rice Institute, Houston, Texas.